Electronics and Electrical Engineering

AIMS Electronics and Electrical Engineering, 9(4): 565–588.
DOI: 10.3934/electreng.2025025
Received: 19 June 2025
Revised: 08 August 2025
Accepted: 08 September 2025
Published: 16 September 2025

https://www.aimspress.com/journal/ElectrEng

Research article

Bald eagle search algorithm based PI control method for speed control of BLDC motor drives

Arwa Amer Abdulkareem[1], Ietiqal M. Alwan[2] and Salam J. Yaqoob[3,*]

[1] Electrical Engineering Technical College, Middle Technical University, Baghdad 10001, Iraq
[2] Renewable Energy Center, Ministry of Electricity, Baghdad 10001, Iraq
[3] Training and Energy Researches Office, Ministry of Electricity, Baghdad 10001, Iraq

* **Correspondence:** Email: engsalamjabr@gmail.com; Tel: +9647819718556.

Abstract: Optimizing the proportional-integral (PI) controllers in brushless direct current (BLDC) motors can improve performance by minimizing the rise time, settling time, and steady-state error. Therefore, a new strategy for speed control for BLDC motors was presented using the bald eagle search (BES) algorithm for optimizing the PI controller. The main objective of this research was to enhance the dynamic performance of the BLDC motor with high efficiency and low steady-state error under load saturation and different operating conditions. The novel speed controller based on the BES–PI methodology is suggested to optimize the controller parameters without the necessity of using the trial-and-error technique. Simulations of the BLDC motor governed by hysteresis current control (HCC) were conducted through the MATLAB/Simulink environment. The obtained results were compared with those achieved using particle swarm optimization (PSO), classical PI, and slide mode control (SMC). The BLDC motor–based BES algorithm showed better robustness, better accuracy for tracking reference speed, and better disturbance rejection than traditional controllers. The average rise time values of the SMC, PI, and PSO-PI techniques were 0.016 s, 0.048 s, and 0.023 s, respectively. In addition, the settling times were 0.61 s for the SMC method, 0.21 s for the PI method, and 0.012 s for the PSO-PI method. Finally, the BES–PI control was the best controller for BLDC motors, with average rise time values of 0.01 s, a settling time of 0.05 s, and no overshoot.

Keywords: PSO; bald eagle search algorithm; speed control; PI controller; BLDC; particle swarm optimization; slide mode control

1. Introduction

1.1. Background

The brushless direct current (BLDC) motor is the most commonly used in industrial and electric vehicle applications due to its low maintenance and high efficiency. However, precise speed control is one of the most crucial issues for BLDC motor control, especially in highly variable operating conditions. There are many challenges regarding precise speed control for BLDC motors, even with all the advantages [1]. These challenges arise from motor nonlinearity, variations of parameters, and even external forces or interference. A major difficulty is due to the motor's back Electromotive Force (EMF) exhibiting a nonlinear region with rotor speed, which leads to low-speed control problems where the back EMF is low. Sudden alterations in load and external interferences are known to cause major speed drift and thus immensely hamper system efficiency. Another issue is the monitoring of the precise rotor angular displacement, which depends on accurate sensing. Hall sensors and encoders are typically incorporated to gauge the rotor position, but these offer a big deal of interference if not misaligned, which occurs in poorly timed commutation and ultimately uncontrollable speeds [2,3]. However, to achieve optimal performance, energy efficiency, and sustainable system stability, speed control is crucial. Traditional approaches, such as proportional-integral derivative (PID) controllers, have been used to regulate the speed [3]. These methods have poor performance under sudden load conditions. For this reason, bio-inspired or metaheuristic algorithms are integrated with the PID controller to improve efficiency and accuracy for the control systems [4–6]. They are capable of recalibrating control parameters and responding to changes in operating conditions, which makes them very appropriate for BLDC motor features. However, implementing a reliable system that accurately controls BLDC motors is critical to achieve high performance and high efficiency under operation [7,8]. BLDC motors have a high application range in crucial areas of modern devices, such as electric vehicles, robotics, and renewable energy systems, where systems need constant and exact control of speed throughout operations. BLDC motors are susceptible to sudden disturbances like abrupt load changes, supply voltage variances, and even changes in normal operating temperature. In the absence of robust controls, these factors will lead to speed oscillations, torque ripples, and instability of the system. The performance degradation of traditional controllers is also caused by the mixing of motor resistance and changes in its inductance. Nonetheless, adaptive robust controls, such as fuzzy logic (FL), model predictive control (MPC), and sliding mode control (SMC) methods, allow for the sustenance of accuracy without constant tuning due to their ability to adjust to shifts in parameters [9,10].

1.2. Literature review

The advancement of industrial automation is steadily enhancing the usage of BLDC motors in construction machinery as well as in power generation equipment. Improving both the static and dynamic characteristics of speed control systems for these motors not only vastly increases the efficiency of the equipment but can also reduce energy consumption. In [11], the authors presented a new PSO-based fuzzy-PID control method as a hybrid approach for optimizing the dynamic noise of the error signal of the BLDC motor speed. This rendered the algorithm vulnerable to system uncertainty and measurement noise coupling during the parameter estimation procedure, resulting in

system performance deterioration. Based on these issues, the current study formulates a framework with a synergistic untraceable Kalman filter (UKF) and PSO fuzzy-PID control for speed control of a BLDC motor. The UKF provides highly accurate estimation data. The PSO is adept at rapidly tuning the fuzzy-PID parameters to address nonlinearity and uncertainty issues during the functioning of diesel engines.

The authors in [12] proposed a fuzzy-PID control scheme to regulate the speed of the BLDC. The research approach was verified through simulation using MATLAB/Simulink. During testing, a speed set-point input of 650 rpm was provided, and the system was tested using two methods, fuzzy-PID logic and the conventional PI method. The findings showed that the overall performance of the fuzzy-PID control was better than that of the conventional PI control. Implementing fuzzy-PID control minimizes both speed fluctuation and torque stability, which enhances BLDC reliability. The research work in [13] proposed a grey wolf optimization (GWO) algorithm, which optimally tuned the parameters of the PID controller. This article aimed to show the difference made by GWO in comparison to the PSO technique and how the results from both approaches differ for tuning the PID controller. The authors in [14] presented a sensor-less BLDC motor using PID and fractional-order (FOPID) control methods. Moreover, tuned parameters provided sufficient regulation for the speed control of the BLDC motor rotor position. In this study, the back EMF, which is produced in the coils, was used to estimate the rotor position. The nonlinearity problem appears when electronic commutators are used in place of traditional motors. To solve this problem, sensor-less BLDC motors are used, and the efficiency and controllability of the closed-loop drives are improved. A novel study evaluated FOPID controllers where the speed of the sensor-less BLDC motors was perturbed outside of their static and dynamic response regions. In addition, the authors in [15] solved the EMF problem through the mathematical formulation of multi-objective optimization problems with constrained differential evolution and PSO-PI controllers. The methodology applied real-time information about the road gradient into the EV control system to increase accuracy and reduce energy utilization. The proposed technique presented a high energy efficiency and precise control of motor speed in EVs by reducing mean square error (MSE) and energy consumption by 95.4% and 3.1%, respectively. Bazi et al. [16] presented a new algorithm called the fast firefly algorithm (FFA), which offered good results in tuning the PID gains for controlling the BLDC motor. Furthermore, an effective control for a BLDC was achieved with high performance under different load conditions. The work in [17] focused on a modified genetic algorithm (MGA), which was developed to tune five parameters of the FOPID controller for speed control of a BLDC motor using a sensor-less method. The MGA is a metaheuristic-inspired algorithm that tackles nonlinearity issues, such as abrupt load changes, and then provides a high response with a small settling time. The MGA-FOPID controller, which combines the modified genetic algorithm and the FOPID controller for BLDC motor's speed control, can better solve problems without using sensors and under changing loads and speeds. The proposed design of the MGA-FOPID controller was implemented using MATLAB/Simulink. The study in [18] focused on investigating the speed control of a BLDC motor based on various control approaches. The first controller was designed as a classical PI controller, relying on adaptive neuro-fuzzy intersection systems known as PI-ANFIS and PSO-PI-ANFIS. The aim was to maintain the rotor speed at the desired set point while mitigating load torque disturbance and parameter changes. The proposed controller was implemented on a dSPACE platform.

A novel approach was presented in [19] to obtain proper BLDC control with the desired specifications. Therefore, a radial basis function neural network (RBFNN) and the student psychology

optimization algorithm (SPOA) were proposed. The RBFNN is trained first, and its output is processed by the SPOA, which also controls the BLDC motor. The RBFNN-SPOA method was investigated to tune the PID parameters. The method was evaluated under different load conditions, taking into account the constraints to minimize the system's objective function. The controller performance was proved in terms of rise time, speed overshoot, settling time, and steady-state error. In [20], an H-infinity control strategy with a PSO algorithm was used for hardware implementation for a sensor-less BLDC motor drive. The applied methodology improved the dynamic response of the BLDC motor using a sensor-less position detection technique. In [21], different optimization algorithms were applied for tuning the PI controller to regulate the speed of the BLDC motor. The effectiveness of the controller was evaluated and gauged through the Integral Square Error (ISE) criteria. Naqvi et al. [22] suggested a multi-objective optimization-based approach to calibrate PI controllers in BLDC motors used in electric vehicles (EVs). Their research targeted two essential objectives: motor speed regulation performance improvement and energy efficiency for supporting sustainable EV operation. These goals were attained by utilizing a constrained swarm-based optimization methodology. The proposed methodology permits adapting a PI controller to changing driving situations to optimize vehicle performance while enabling the reduction of energy.

The authors in [23] proposed a heuristic adaptive lyrebird optimization algorithm for adapting PI controllers used in BLDC motors. The research placed particular focus on improving the dynamic response of the motor, specifically speed variations under changing torque conditions. The lyrebird optimization algorithm is an innovative approach to solving the unique requirements of the system, making it more efficient when tuning compared to traditional methods. Therefore, the adaptive tuning process enables faster response times and increased stability, especially in applications involving changing load conditions. Çelik and Karayel [24] proposed an innovative solution to overcome the dynamic and crucial function of the BLDC motor speed control. The remarkable accomplishment was realized successfully by combining the sophisticated characteristics of a snake optimizer with a fractional-PI controller's cascading structure. It provided a very effective solution for improving the speed regulation of the motor. This improvement was achieved by successfully decoupling all of the different control loops, which in turn contributes to improved response times in motor control. These improvements not only yield improved dynamic performance but also lead to smoother running of the motor, which are invaluable characteristics. The research results show that this innovative control using the snake optimizer resulted in considerably more accurate speed regulation. The authors in [25] presented a whale optimization algorithm (WOA) to determine the optimal gains of the PID controller. Findings demonstrated that the suggested algorithm significantly enhanced speed regulation of the motor and increased accuracy in terms of settling time and speed overshoot. The applied method not only improved the performance of the BLDC motor but also contributed to energy consumption. This process can provide an attractive solution with precise speed control for EV applications. The researchers in [26] conducted a cuckoo optimization algorithm (COA) to optimize a fuzzy logic controller, which was specifically implemented for BLDC motors. However, the results drawn from this study pointed to significant improvements in the ability to remarkably improve fuzzy controller performance by allowing very accurate adjustments of its parameters. Moreover, the hybrid technique improved the motor speed regulation, significantly reduced steady-state errors, and overall improved adaptability, most significantly when dealing with dynamic operating settings. Finally, the fuzzy controller based on COA further exhibited distinguished ability to accurately handle load fluctuations

and uncertainties, thereby presenting a measure of ruggedness and performance significantly better compared to the PID method.

The study in [27] focused on optimizing a PI controller in a class topper optimizer (CTO) algorithm; this research strived to realize a myriad of very significant objectives. These include achieving improved speed control, reducing steady-state error, and improving dynamic responses, each forming a vital role in ensuring the effective operation of electric vehicles. Therefore, the PI controller is being optimized very carefully, and this is accomplished with this algorithm. The CTO method is a very advanced and highly innovative technique, specifically developed with the purpose of optimizing and improving the performance levels of typical control systems, like the PI controller. Moreover, the optimized PI control allows for improved response times and better adaptability to varying load and speed conditions in sensor-less BLDC motor drives. Poudel and Bhandari [28] proposed a novel and innovative control method by presenting the use of the ant colony optimization (ACO) algorithm to optimize the PID controller parameters for controlling the speed of the BLDC motor. The general focus of their research work was to improve the performance characteristics of the motor by meticulous and detailed tuning of the PID parameters, aiming to enhance the response time and stability. The ACO algorithm draws its inspiration from modeling the natural and innate searching behavior of ants in their natural habitat, thereby providing an extremely efficient and adaptable algorithm to be utilized to optimize controllers' parameters. The testing of this method shows an improvement in motor speed regulation performance in terms of the standard of minimum overshoot, reduction of steady-state error, and reduction of settling times.

The authors in [29] proposed an FOPID controller to regulate the BLDC motor speed and minimize the overshoot and settling time in the classical PI methods. The design architecture of this superior controller was carefully designed with particular emphasis upon allowing the greatest possible efficiency of speed control performance. This promising breakthrough has been rigorously optimized and carefully developed step-by-step through the application of the pelican optimization algorithm (POA). The overall objective of the paper largely centered around improving motor driving performance through employing a hybrid form of control strategy that efficiently combines various fractional-order approaches with well-proven conventional standard control methodologies, such that it develops an integrated and effective control approach. The results showed that the used controller achieves a remarkable superiority over conventional PI controllers in many critical aspects, including robustness, stability, and energy efficiency. In [30], a new transit search optimizer (TSO) technique was proposed to optimize the PID controller-based BLDC motor drive system. The main objective was to considerably optimize the control performance in relation to the motor speed, as well as to optimize general dynamic performance potential in real-world applications. By improving the motor's response, the overshoot in its speed was avoided. The authors recommended using this algorithm as a sophisticated optimization technique to adjust PID controller parameters. Moreover, using the TSO optimizer can optimize the critical parameters that exist within the controller, including the proportional, integral, and derivative gains, while also considering the distinct operating characteristics and behaviors of the particular target motor. Therefore, with this sophisticated and innovative technique, a much more accurate and effective motor control system is finally achieved.

1.3. Research contributions

The contributions of the proposed article are:

i. This paper introduces an innovative optimization method called the bald eagle search algorithm to control the BLDC motor speed. Therefore, it aims to boost and maximize the overall performance and efficiency of the entire motor drive system.
ii. The BES-based PI controller improves the transient response of the BLDC motor, providing faster settling time and minimizing overshoot.
iii. By optimizing the PI parameters using BES, the system exhibits a greater reduction in steady-state speed error. This enhancement improves the motor's precision and maintains the reference speed within its range under various operating conditions.
iv. The proposed study provides significant insights into real-world motor applications. The suggested control can be applied in EVs and other systems that need a high-performance BLDC motor drive.

1.4. Organization of research

The rest of this paper is organized as follows: Section 2 presents the mathematical analysis of the BLDC motor. Section 3 introduces the control system of the BLDC motor. Section 4 introduces results and discussion, and Section 5 presents the conclusion of the paper.

2. Mathematical analysis of the BLDC motor

The three-phase voltage ($v_{an}, v_{bn},$ and v_{cn}) equations of the BLDC motor can be written as follows [31]:

$$v_{an} = R_s i_a + \frac{d}{dt}(L_a i_a + M_{ab} i_b + M_{ac} i_c) + e_{an} \tag{1}$$

$$v_{bn} = R_s i_b + \frac{d}{dt}(L_b i_b + M_{ba} i_a + M_{bc} i_c) + e_{bn} \tag{2}$$

$$v_{cn} = R_s i_c + \frac{d}{dt}(L_c i_c + M_{ca} i_a + M_{cb} i_b) + e_{cn} \tag{3}$$

These equations can be written in matrix form:

$$\begin{bmatrix} v_{an} \\ v_{bn} \\ v_{cn} \end{bmatrix} = R_s \begin{bmatrix} i_{an} \\ i_{bn} \\ i_{cn} \end{bmatrix} + \begin{bmatrix} L_a & L_{ab} & L_{ac} \\ L_{ba} & L_b & L_{bc} \\ L_{ca} & L_{cb} & L_c \end{bmatrix} \frac{d}{dt} \begin{bmatrix} i_{an} \\ i_{bn} \\ i_{cn} \end{bmatrix} + \begin{bmatrix} e_a \\ e_b \\ e_c \end{bmatrix} \tag{4}$$

where R_s is the phase resistance, and i_a, i_b, and i_c are the currents of the phases a, b, and c, respectively. L_a, L_b, and L_c represents the self-inductances of the phases, and $M_{ab}, M_{ac}, M_{ba}, M_{bc}, M_{ca}, and\ M_{cb}$ are the mutual inductance between the motor's phases. In BLDC motor design, the phases of the motor in stator winding are symmetrical. As a result, the Equations (5–7) are written as follows:

$$R_a = R_b = R_c = R_s \tag{5}$$

$$L_a = L_b = L_c = L \tag{6}$$

$$M_{ab} = M_{ba} = M_{ac} = M_{ca} = M_{bc} = M_{cb} = M \tag{7}$$

Using this assumption in phase voltages equations (1–3) yields the new formulas [21]:

$$v_{an} = R_s i_a + \frac{di_a}{dt}(L - M) + e_{an} \tag{8}$$

$$v_{bn} = R_s i_b + \frac{di_b}{dt}(L - M) + e_{bn} \tag{9}$$

$$v_{cn} = R_s i_c + \frac{di_c}{dt}(L - M) + e_{cn} \tag{10}$$

In BLDC motor representation, the EMFs with trapezoidal waveforms can be expressed as presented in the equations below [31]:

$$e_a = K_e\ \omega_m\ f_a(\theta_e) \tag{11}$$

$$e_b = K_e\ \omega_m\ f_b(\theta_e) \tag{12}$$

$$e_c = K_e\ \omega_m\ f_c(\theta_e) \tag{13}$$

where K_e is the voltage constant, ω_m represents the mechanical speed in rad/s, and $f_a(\theta_e)$, $f_b(\theta_e)$, and $f_c(\theta_e)$ are the three-phase trapezoidal wavers of unity magnitudes [21]. However, the BLDC motor torque (electromagnetic torque) can be written as follows [31]:

$$T_{em} = \frac{(e_a\ i_a + e_b\ i_b + e_c\ i_c)}{\omega_m} \tag{14}$$

The electromagnetic torque is written as follows:

$$T_{em} = T_L + J_m \frac{d\ \omega_m}{dt} + B\ \omega_m \tag{15}$$

where J_m is the mechanical friction and B is the motor's inertia.

3. Control system of the BLDC motor

3.1. PI control

The block diagram of the suggested system is shown in Figure 1. In this study, hysteresis current control has been utilized because of its simplicity and fast dynamic response; it is widely used for the regulation of BLDC motors. This control method ensures that the current of the motor stays within specified limits by comparing the motor's actual current and a specified reference value. Therefore, this approach requires the soft switching of the DC/AC converter to maintain the motor's current within its limits, especially under load torque disturbances. Thus, hysteresis current control enables stable motor operation with minimal torque fluctuations, making it especially suitable for use in robotics and electric vehicles, where smooth operation is essential [32]. However, the PI controllers implemented in BLDC motors have limitations that can be addressed with metaheuristic optimization algorithms. While many systems can function well with PI controllers, they tend to be sensitive to parameter changes, have poor dynamic response, and are difficult to adapt to different operating conditions. Additionally, these algorithms fine-tune controller parameters to solve issues, which enables enhanced motor functioning. Moreover, with the proper PI gains achieved, the motor system performs efficiently with a strong response and offers minimal oscillation. The PI control equation can be written as follows [33]:

$$u(t) = k_p.e_{ss}(t) + k_i \int_0^t e_{ss}(\tau)d\tau \tag{16}$$

where $u(t)$ is the PI control output, k_p is the proportional gain, k_i is the integral gain, and $\int_0^t e_{ss}(\tau)d\tau$ represents the integral of error over time.

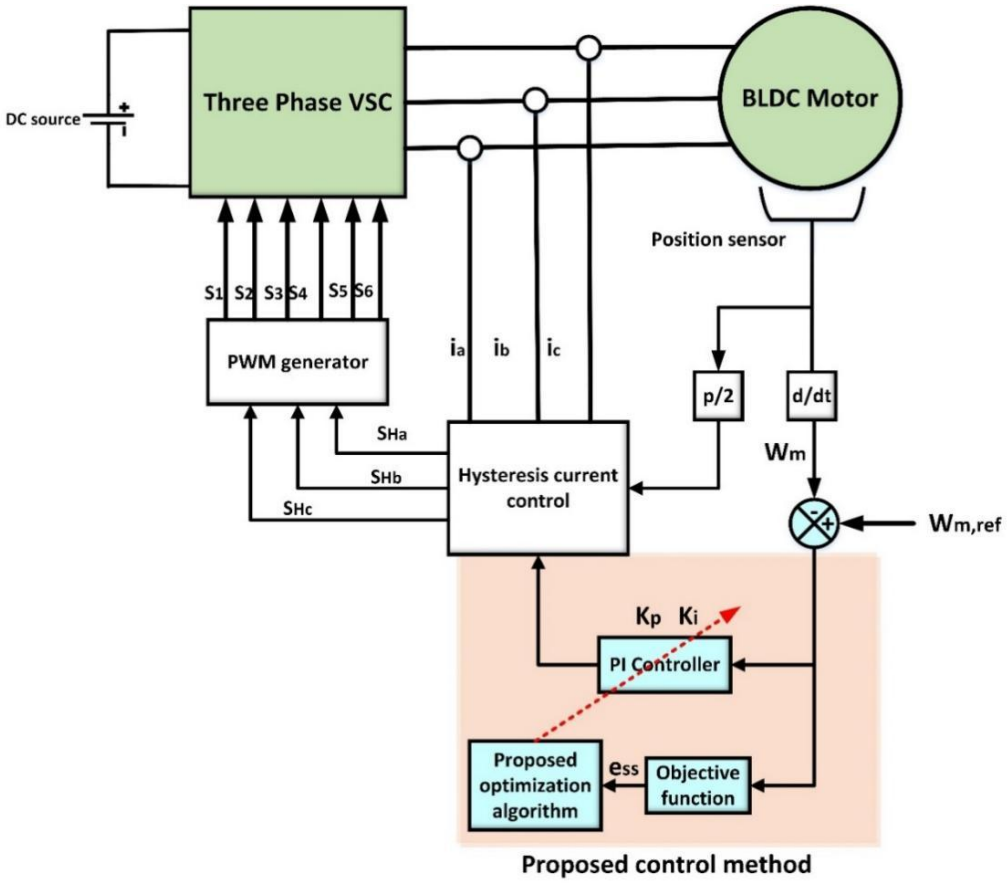

Figure 1. Block diagram of the proposed system.

3.2. Proposed objective function

The steady-state error is the objective function that is tracked by the PI controller. Moreover, the suggested objective function is the integral square error (ISE) that can be written as follows:

$$ISE = \int {e_{ss}}^2 (t)dt \tag{17}$$

where e_{ss} is the steady-state error that can be written as $e_{ss} = \omega_{m,ref} - \omega_m$, where ω_m and $\omega_{m,ref}$ are the speed of the motor and the reference speed. The PI gains are estimated based on the ISE value. The k_p and k_i bounders are limited as follows:

$$\begin{cases} k_{p,min} < k_p < k_{p,max} \\ k_{i,min} < k_i < k_{i,max} \end{cases} \tag{18}$$

where $k_{p,min} = 0.1$, $k_{p,max} = 10$, $k_{i,min} = 2$, and $k_{i,max} = 50$.

3.3. The bald eagle search (BES) algorithm

3.3.1. Overview of BES

The BES algorithm is a nature-inspired heuristic optimization technique that imitates the

hunting process of a bald eagle [34,35]. Bald eagles hunt through an exploration, exploitation, and swooping process. The eagle searches for opportunities in wide spaces in the exploration phase; in this stage, measures are taken to make sure that there is no early restriction on the process. Moreover, when there is a high possibility of getting an eagle, the depletion stage starts. In this stage, the eagle furthers their local search, or in other words, narrows the area of focus to increase efficiency. Lastly, the eagle eliminates their target during the precise attack, and this leads further to an optimal output. The implementation of BES provides a good balance that is both local and global, thereby ensuring that optimization issues are solved [34]. BES is more effective in areas such as engineering optimization, renewable energy systems, and machine learning, which require attention when it comes to solving complex nonlinear and multidimensional problems. The hunting behavior of BES is shown in Figure 2.

3.3.2. Initialization of the algorithm

The BES can find optimal solutions by creating random initial populations within the limits of candidate solutions. Consider that there are populations N, each containing d_{min} of the decision variables. The formulated random population is created using the following equation [34]:

$$P_i^j = L_B + rand \times (U_B - L_B) \quad \begin{cases} i = 1,2 \dots \dots, N \\ j = 1,2, \dots \dots, d_{min} \end{cases} \tag{19}$$

where $rand$ represents a random number [0,1], U_B represents the upper limits, L_B is the lower limits, and P_i^j represents the position of the j-th dimension in the i-th population.

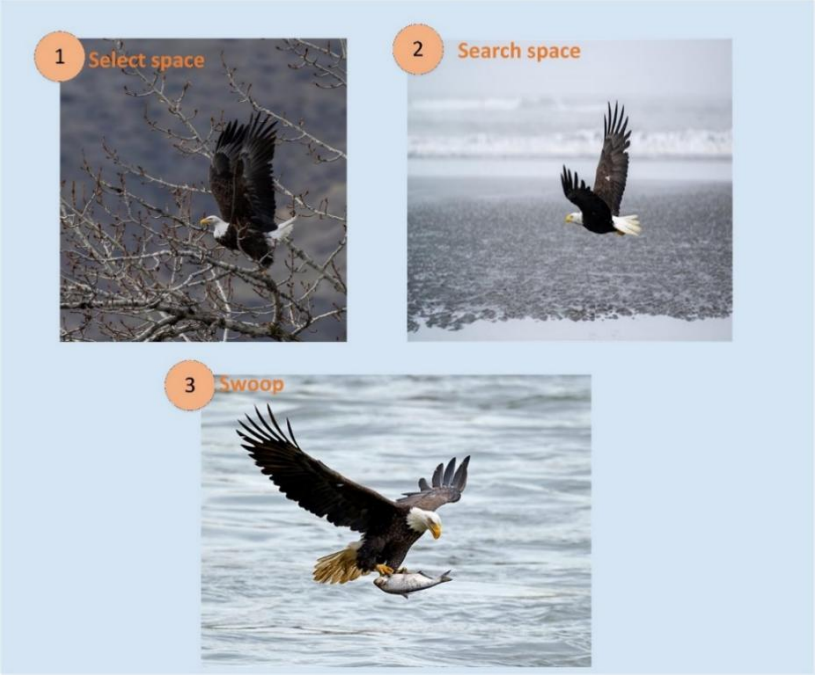

Figure 2. Bald eagle during the hunting process.

3.3.3. Space selection

In selecting search areas and assessing quantities of prey to decide the best site to target, bald

eagles display random search behavior. In this step of the BES algorithm, the current location of the bald eagle, $P_{i,new}$, is generated through a random search with a scale of prior information and a factor of α. The random search operations can be defined mathematically in the following way [34,35]:

$$P_{i,new} = P_b + \alpha \times R_{rand} \times (P_m - P_i) \quad (20)$$

where α represents the response control action, P_b is the existing best position, P_m specifies the mean distribution position of the eagles, R_{rand} is the random number [0,1], and P_i is the position of the i-th bald eagle.

3.3.4. Space searching

Once an eagle locates a suitable spot, it adjusts its movement for more detailed searches. In the searching for prey phase, eagles look for their prey in the previously selected areas, and this process of hunting improves the overall search. A behavioral analysis of this activity can be given by the following equations (21–24):

$$P_{i,new} = P_i + x(I) \times (P_i - P_m) + y(I) \times \quad (P_i - P_{i+1}) \quad (21)$$

$$x_i = xr_i / \max(|xr|), y_i = yr_i / \max(|yr|) \quad (22)$$

$$xr_i = r_i . \sin(\theta_i), yr_i = r_i . \cos(\theta_i) \quad (23)$$

$$r_i = \theta_i + a \times R_{rand}, \theta_i = b \times \pi \times R_{rand} \quad (24)$$

where x_i and y_i are the coordinates of the eagle's location, and a and b are the random numbers for estimating the spiral trajectory.

3.3.5. Swooping process

The swooping stage of the BES algorithm is the last step wherein the search agents (eagles) move toward the best solutions located so far with great accuracy. This phase guarantees rapid convergence as well as optimal solution refinement [34]. The state of motion is articulated mathematically with the help of polar coordinates as shown in Eqs. (25–28):

$$P_{i,new} = R_{rand} \times P_b + x_{1i} \times (P_i - c_1 P_m) + y_{1i} \times (P_i - c_2 P_b) \quad (25)$$

$$x_{1i} = xr_i / \max(|xr|), y_{1i} = yr_i / \max(|yr|) \quad (26)$$

$$xr_i = r_i . \sinh(\theta_i), yr_i = r_i . \cosh(\theta_i) \quad (27)$$

$$r_i = \theta_i, \theta_i = b \times \pi \times R_{rand} \quad (28)$$

where x_{1i} and y_{1i} are the locations of the eagles in the polar coordinates, and c_1 and c_2 are the random numbers of the level of motion of bald eagles in the direction of optimal and mean locations, respectively. Figure 3 shows the flowchart of the BES algorithm.

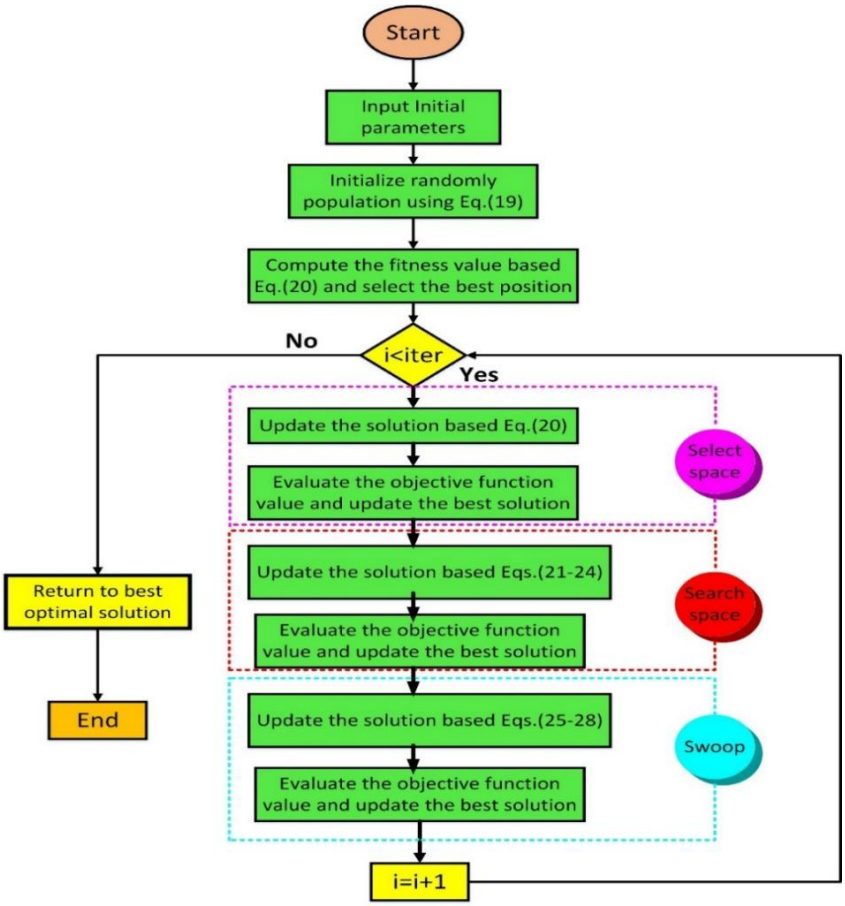

Figure 3. Flowchart of the BES algorithm.

4. Results and discussion

4.1. Evaluation and case studies

The results of the simulation are obtained via MATLAB/Simulink as displayed in Figure 4. As observed, the used model consists of a DC/AC converter with a DC bus voltage of 310 V, a 300 W BLDC motor, and HCC controller blocks. Table 1 displays the parameters of the BLDC motor. Table 2 shows the parameters of the BES and PSO algorithms used in this work.

The speed controller using BES–PI was investigated to regulate the reference current that was used as input to the hysteresis-based current controller. The proposed method was tested under different case studies. The first case study was conducted with rated torque and a step change in the motor's speed. In case 2, the rated torque was applied to the motor with different steps in the motor's speed. The third case used a step change scenario in the load torque-based rated speed value. The case studies are discussed below.

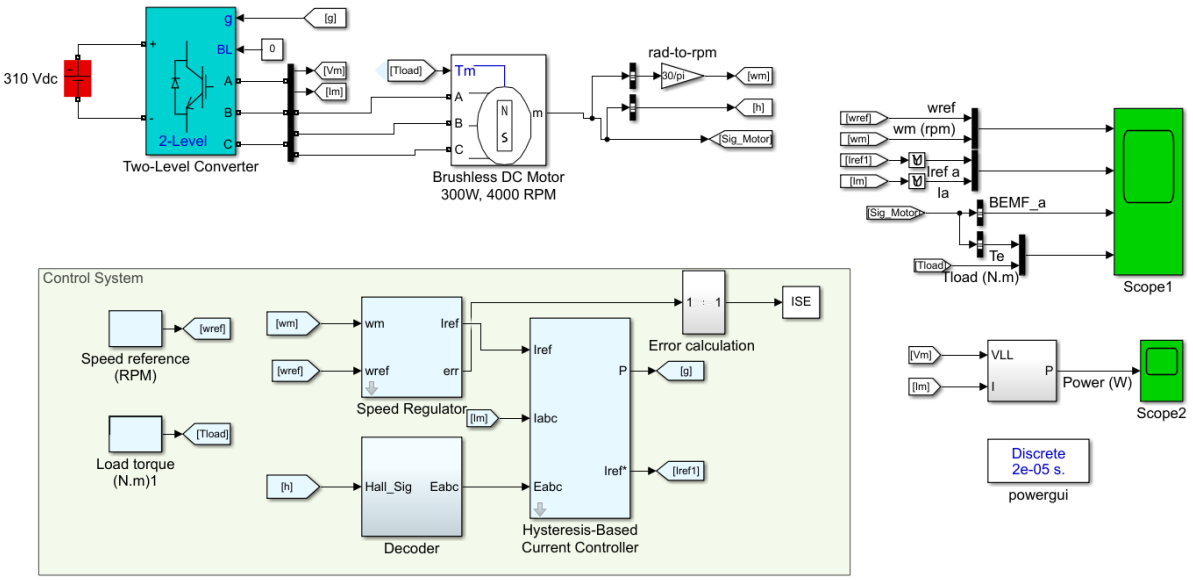

Figure 4. Simulink model of the proposed system.

Table 1. Parameters of the BLDC motor.

Parameter	Value
R_s	8.3 Ω
L	19.5 mH
K_e	146 V
J_m	$1 \times 10^{-4}\ Kgm.m^2$
B	1×10^{-2} N. m. s
Pole pairs	4

Table 2. Parameters of the BES and PSO algorithms.

Algorithm	Parameter	Value
BES	Search agents	10
	Max. iterations	100
	L_B	0
	U_B	50
	C_1 and C_1	[0,1]
	d_{min}	2
PSO	Search agents	15
	Max. iterations	100
	L_B	0
	U_B	50
	C_1 and C_1	0.2
	w	0.9

- **Case 1: Rated torque with a step change in the motor's speed**

In this section of the results and validation, the motor's torque remains constant at 0.7 N m.

Moreover, the speed of the motor is changed from 4000 to 1000 RPM after 1 s of the simulation. The step change in the reference speed can clarify the robustness of the controller. As illustrated in Figure 5, the motor speed response nearly follows the reference speed, achieving steady-state operation at approximately 4000 RPM before experiencing a sharp deceleration at approximately 1 second. This indicates a well-tuned speed control loop. Figure 5(b) shows the stator current and its reference, where initially the currents are quiescent and stable during the steady-state portion. As observed, after the speed drop, the current begins to ripple with increased oscillation, illustrating the motor's struggle to adapt to the new load or operating conditions. In Figure 5(c), the back electromotive force (BEMF_a) exhibits typical sinusoidal waveforms characteristic of BLDC motors under normal operation. After 1 s, the BEMF signal drastically loses amplitude, which, due to the reduction in speed, indicates proper BEMF behavior in relation to motor velocity. Figure 5(d) shows the electromagnetic torque (Te) and load torque (Tload); during steady-state operation, Te captures Tload, demonstrating good torque tracking efficiency. The previously described sharp drop in load torque around 1 s also corresponds with the quasi-steady-speed transition. This distinctly illustrates the controller's response to a dynamic reduction in speed and load capacity. After this disturbance, the torque rapidly settles, illustrating good dynamic performance and torque stability.

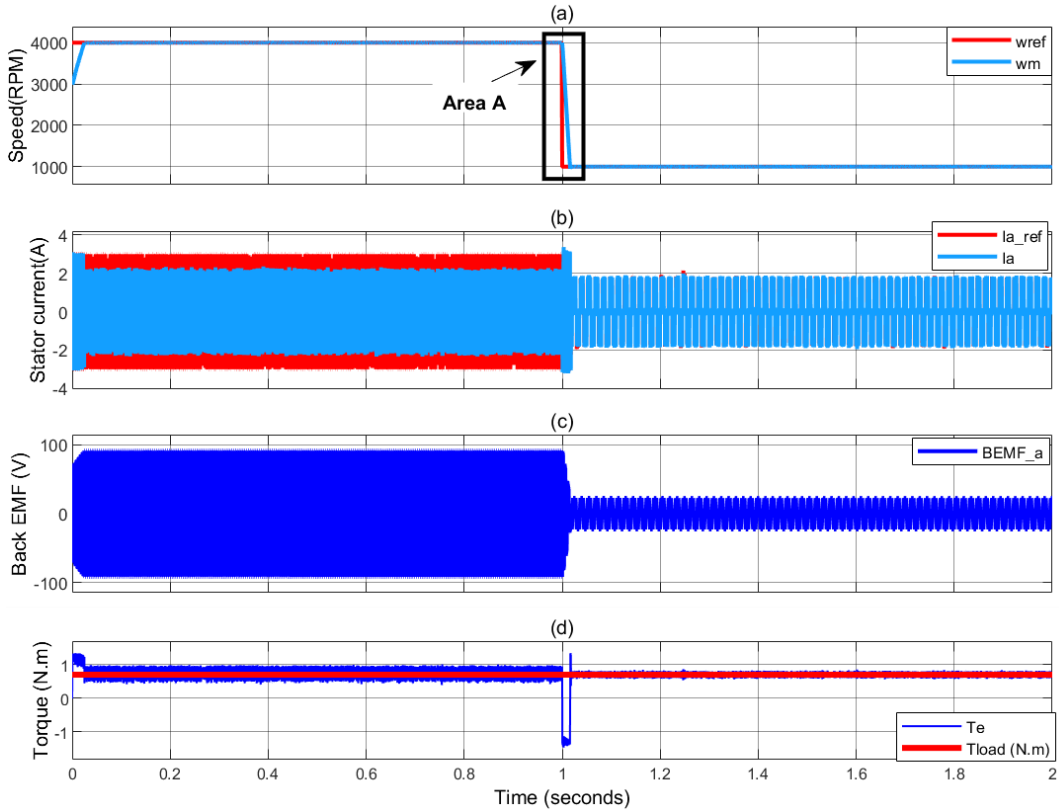

Figure 5. Obtained results for case 1. (a) Motor speed. (b) Stator current phase a. (c) Back EMF of phase a. (d) Torque of the motor.

From Figure 6, it can be seen that the actual rotor speed (wm) tracks the reference speed with high accuracy. At the start, the motor is set to run at a constant reference speed of 4000 RPM. At the time of t ≈ 1.0 s, the motor is commanded to drop the reference speed to zero. Actual speed follows suit smoothly and decelerates to zero, which attests to the effectiveness of the speed controller. The controlled deceleration indicates the capability of the braking system, which tends to be regenerative

braking. In Figure 6(b), the stator phase current (ia) is presented together with its reference (ia_ref). Prior to the deceleration event, the BLDC current is at its pre-deceleration stage for the current buildup, which follows a trapezoidal shape. Furthermore, current tracking has been proven to associate with robust current regulation. Lowering the speed command results in the amplitude of the current also being lowered. Moreover, the current waveform is flat as the rotary motion is near stasis, confirming proper control performance under low-speed and zero-speed conditions.

The back EMF of phase A is shown in Figure 6(c). At high speeds, BEMF exhibits a distinctly trapezoidal pattern, which is characteristic of a BLDC motor. As the motor decelerates, the BEMF reduces in both amplitude and frequency values. This behavior corroborates the relationship between BEMF and rotor speed, thereby affirming the efficacy of proposed control applications. The electromagnetic torque and load torque are presented in Figure 6(d). For the steady state, which persists up until t = 1.0 s, this torque is equal to the constant load torque but with a slight ripple undershoot, indicating satisfactory control of the torque. Upon speed command reduction, the motor shortly acts to produce negative torque as regenerative braking. Furthermore, the results prove that the control system of the BLDC motor seamlessly follows the speed command, maintains constant current for each phase, and reacts appropriately. The lack of abrupt changes in the level of torque and current reinforces the ease with which the control strategy of PI-BES is executed, suggesting smooth operation of the stabilized control system.

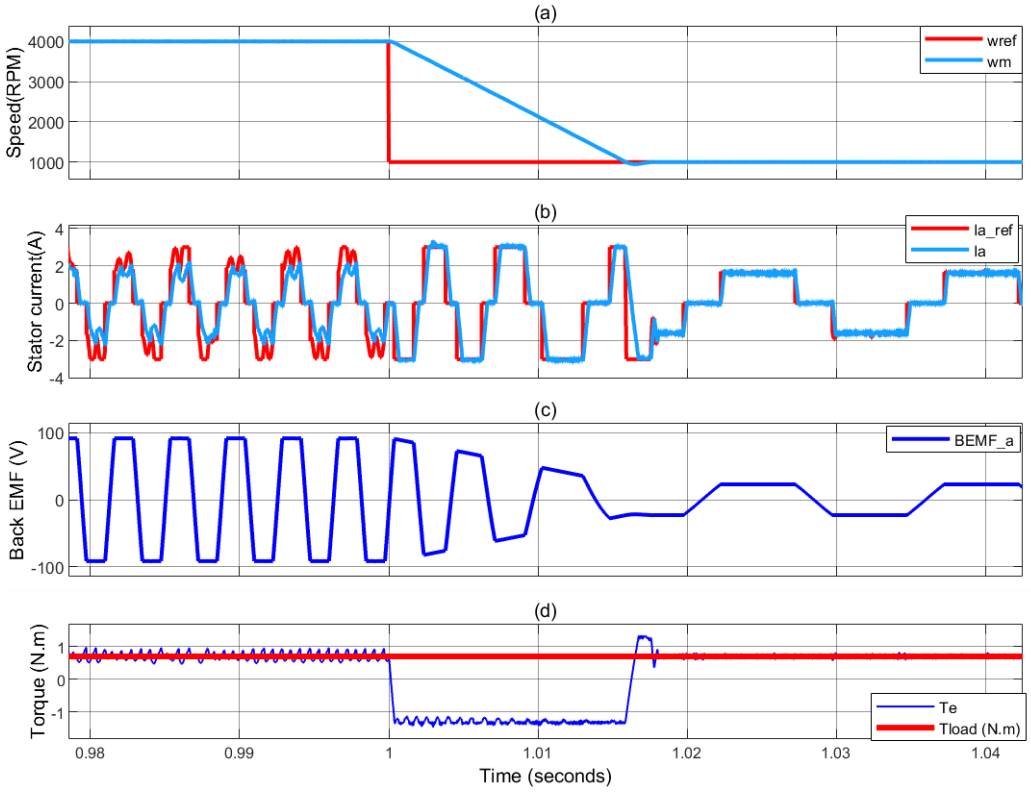

Figure 6. Zoom of the results at case 1.

- **Case 2: Rated torque with different steps in the motor's speed**

In this section, the different steps in the actual motor speed were conducted as shown in Figure 7. It displays the adaptive response of a BLDC motor system to changes in reference speed using the proposed control method. Figure 7(a) shows the motor capsule performing with a reference speed

equal to 3000 RPM. Initially, at time 0.4 s, a stepwise deceleration command is executed. This command sets the reference speed to zero. The actual speed of the motor closely follows the command and reaches a standstill with no overshoot or oscillation. At 1 s, the reference speed is again commanded to increase to 2500 RPM, and the motor responds with rapid acceleration, settling at the new set-point in 80 ms. The performance illustrates that the suggested controller provides a fast response and fewer dynamic transitions.

The corresponding stator current response can be seen in Figure 7(b), where actual and reference currents are plotted for comparison. Current phasing has a value of ±4 A, and the current's trapezoidal reference waveform is suitably tracked during normal operation. During this condition, the motor current always returns to the rated level, aiding torque production. Tracking performance despite some visible noise throughout the waveform is still overall satisfactory, regardless of this case. The BEMF waveform is trapezoidal shaped with an amplitude of approximately 100 V when the motor is not moving. As the motor decelerates, BEMF drops to near zero and rebuilds to around -85 V when the motor resumes motion at 2500 RPM. This is further confirmation of the coupling between rotor speed and BEMF voltage. It also shows that the motor is functioning properly in a sensor-less mode. Load torque remains approximately at 1.1 N ṁ. The constant BEMF indicates load torque. The motor keeps the torque balanced in the system during steady-state operation. In transition-mode speeds, a negative torque spike due to regenerative braking appears at t ≈ 0.4 s, and a positive torque spike settles near 2 N ṁ during re-acceleration. Figure 8 shows the zoom results of case 2.

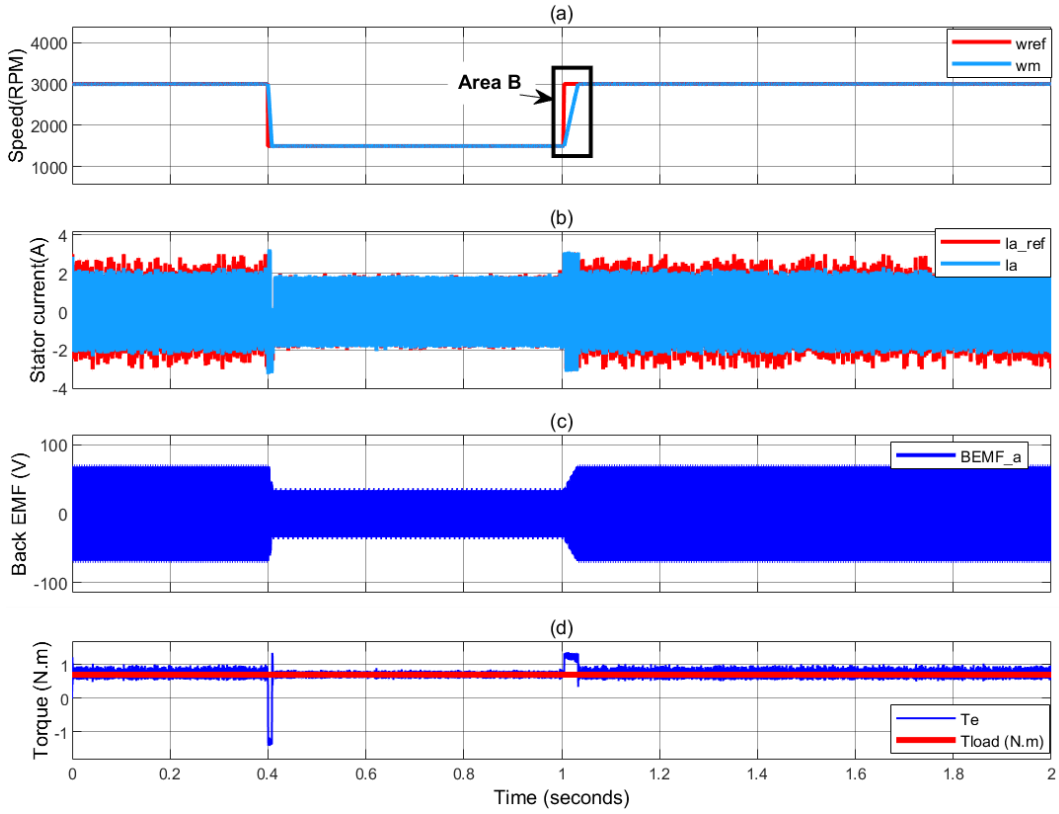

Figure 7. Obtained results under case 2. (a) Motor speed. (b) Stator current phase a. (c) Back EMF of phase a. (d) Torque of the motor.

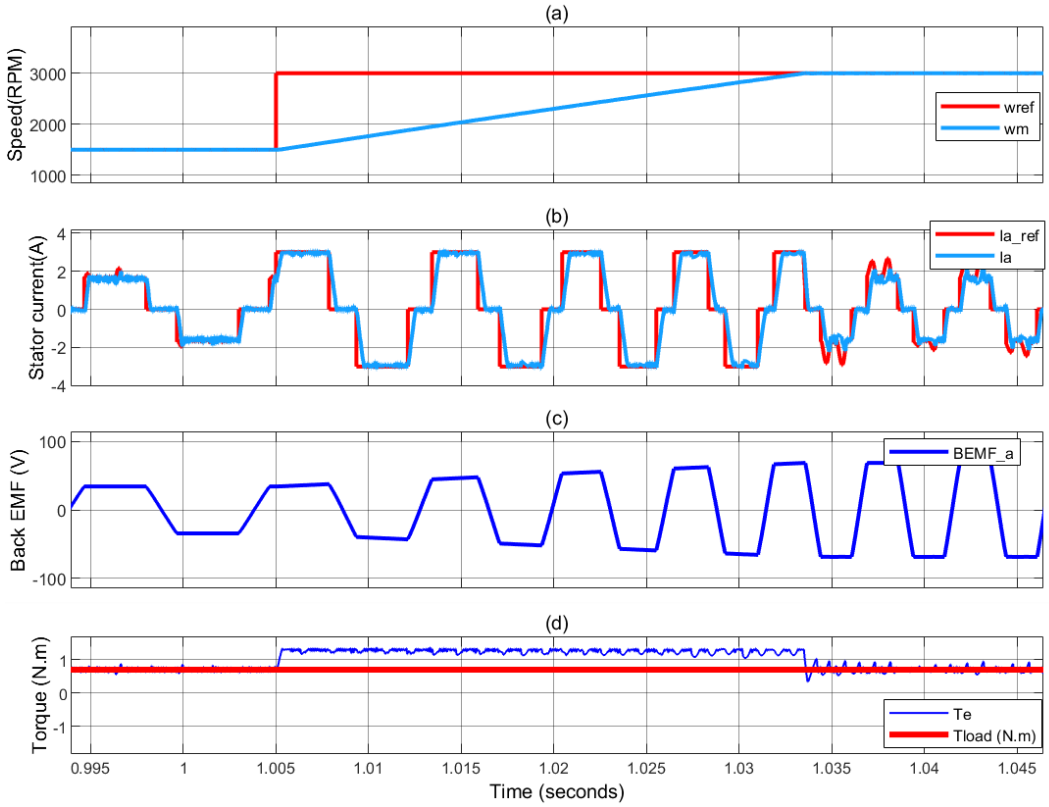

Figure 8. Zoom results of case 2.

- **Case 3: Step change in load torque and rated speed**

The constant reference speed of the BLDC motor is shown in Figure 9. In this case, the variable torque load characteristic was considered. In Figure 9(a), the reference speed is held constant at about 4000 RPM for the duration of the simulation, while the actual rotor speed tracks the set point with a small steady-state error and delay. Even in Figure 9(b), the captured stator current reveals dynamic changes accompanying changes in load. At a light load configuration, the phase current oscillates at ±1.5 A. At around 0.5 s, the system hits a higher load, and this is represented by an increased current of nearly ±3.5 A. After 1.5 s, the load drops, which leads to a reduction of the current level. During the entire operation phase, the current reference follows exactly the current pulse envelope module of the signal, which means an accurate current control and small errors under dynamic movements.

The back EMF curve of phase A is displayed in Figure 5(c). As observed in this figure, the back EMF waveform remains trapezoidal shaped with an amplitude of approximately ±100 V, which suggests that the motor speed is stable. Finally, Figure 5(d) provides a comparative analysis of electromagnetic torque with load torque. At the beginning, both torque values are centered at 1.1 N ṁ. At time t ≈ 0.5 s, T_{load} is stepwise increased, which results in Te also increasing to a peak value of approximately 2.3 N ṁ to satisfy the demand. This load condition persists until roughly 1.5 s, where T_{load} experiences a step reduction. The zoom results are shown in Figure 10, which displays the dynamic response of the motor.

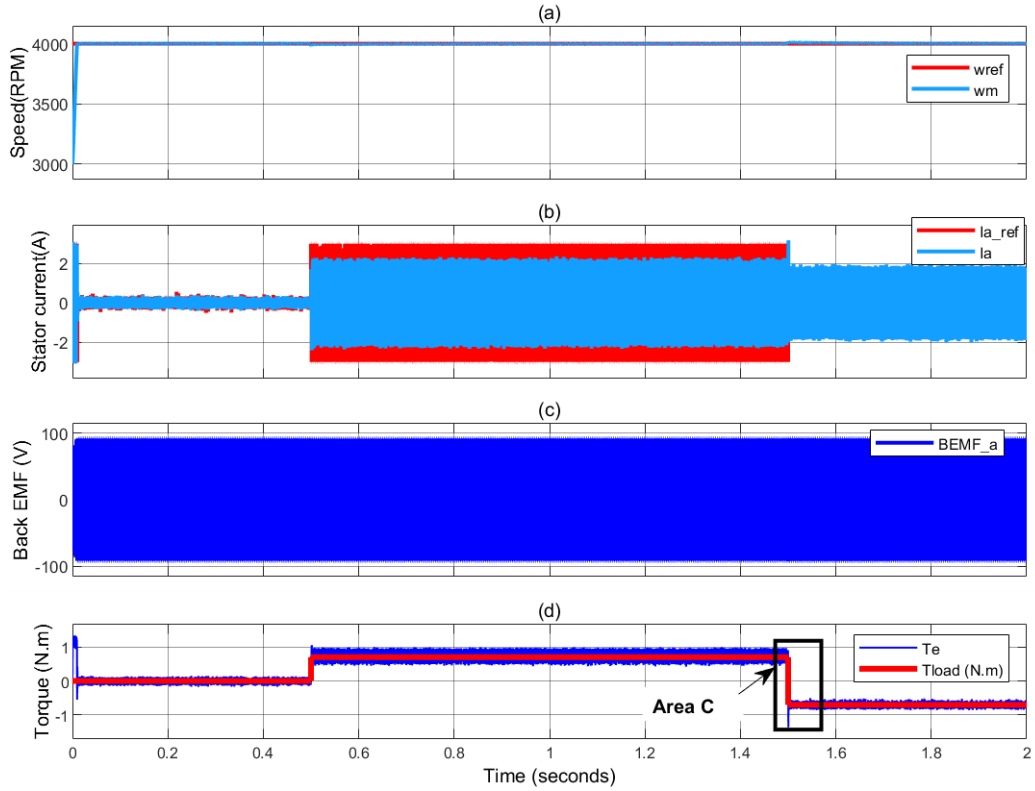

Figure 9. Obtained results of case 3: (a) motor's speed, (b) stator current phase a, (c) back EMF of phase a, and (d) torque of the motor.

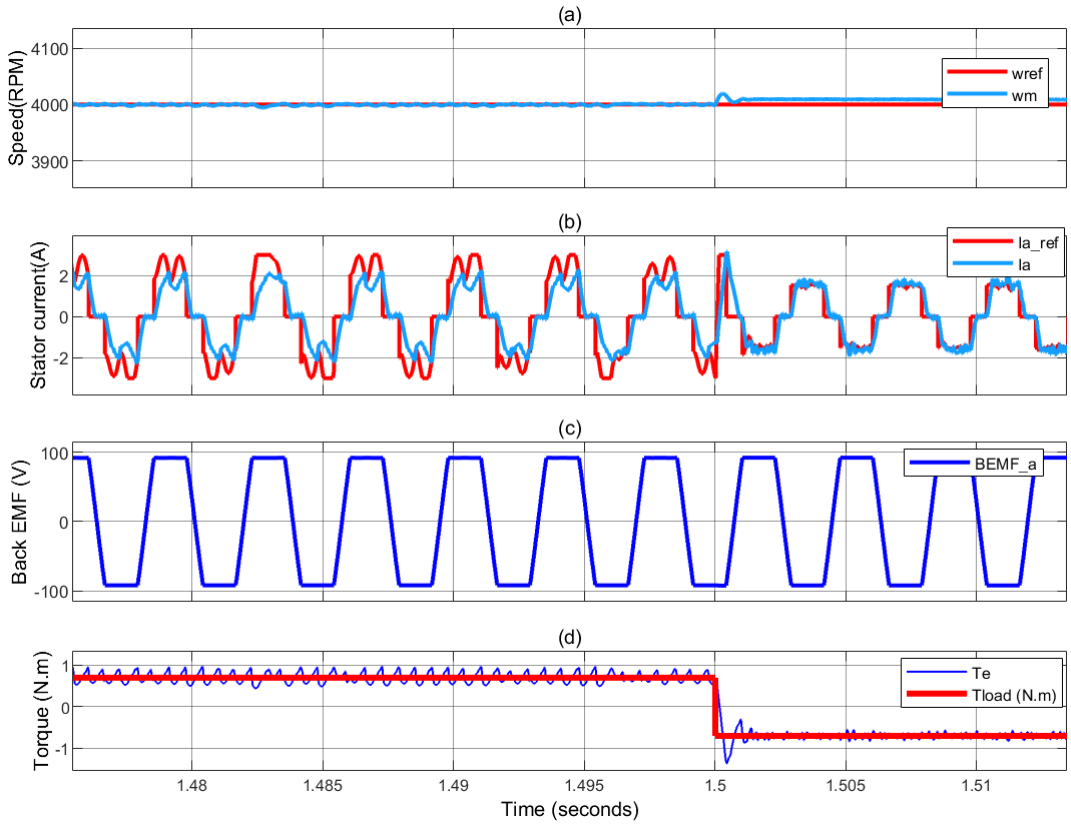

Figure 10. Zoom results of case 3.

4.2. Comparison and assessment

To clarify the novelty of the applied control method, a comparison between the used PI–BES algorithm and other methods is conducted. The proposed method was verified under different speed control methods. The achieved results were compared with the SMC technique, which was implemented in [36], and that enhanced the dynamic performance of the BLDC motor as well as its stability while minimizing chattering in uncertain and nonlinear operating environments. Also, the speed curve results obtained for the case studies are compared with the classical PI control technique in [37] and the PSO-PI control method in [38].

The comparisons of cases 1, 2, and 3 are shown in Figures 11–13, respectively. Figure 11 shows the main results from evaluating the proposed control strategy against three benchmark controllers. The motor is initially commanded to operate at 4000 RPM and then subjected to a disturbance in the form of a speed step drop at t = 1 s. All methods are evaluated on tracking accuracy and disturbance rejection capabilities. In the first zoomed-in area (left inset), which focuses on the start-up behavior, the proposed method presents a remarkably fast convergence (no overshoot or extremely short settling time). On the other hand, the PI controller suffers from significant oscillations and the worst damping out of the methods. The PSO-PI controller is better than the classical PI method due to its reduced speed overshoot with faster settling time. Although this method is still slower than the proposed method, it provides an acceptable response. The SMC controller also demonstrates less overshoot and better convergence, but it suffers from more switching noise, which is considered less efficient compared to the BES–PI method. In the second inset (right), which zooms in on the time interval t = 1 s, the robustness of all methods can be observed. As a result, when the reference speed drops to nearly 1500 RPM, the BES–PI method immediately adapts, showing no sign of oscillation. In contrast, the PI controller suffers from considerable oscillations that dip below -1000 RPM before recovering and returning to the new set point. In addition, the PSO-PI controller overshoots before stabilizing; however, this is an improvement on PI. The SMC presents a decent transition but responds more slowly than the proposed technique and exhibits chattering. Figure 12 shows the comparison under case 2. As observed in this figure, the proposed PI-BES method minimizes overshoot, rise time, and settling time during start-up and step changes in reference speed. With regard to performance, classical PI-PSO or SMC controllers demonstrate overshoot because of aggressive gain settings or an underactive, sluggish response due to conservative tune settings. In contrast, BES-tuned gains are balanced in responsiveness and stability. Figure 13 displays the results of case 3. These results show that the rise time and settling time of the suggested method are better than those of the existing methods. The undershoot in the classical method may damage the motor and limit the speed range.

In summary, the proposed controller outperformed both traditional SMC and PSO-PI metaheuristic-enhanced controllers by the greatest margin in overshoot suppression, achieving a faster settling time and providing a smoother transient response. With all these features combined, the proposed controller displayed its powerful precision and robust dynamic speed control capabilities amid volatile operating conditions. The numerical results of these cases are listed in Table 3.

The results achieved with the BES algorithm can be analyzed as follows:

- ✓ Dynamic response: The optimized PI controller-based BES presents a significantly quicker response time in terms of rise and settling time when compared with other traditional methods.

The rise and settling times in case 1 of the BES method are 0.01 and 0.05 s, respectively; those in case 2 are 0.012 and 0.06 s, and 0.01 and 0.03 s for case 2. The average value of the rise time for the BES is 0.01 s. The average settling time is 0.046 s. As observed in this table, the average values of the rise time for the SMC, PI, and PSO-PI methods are 0.016, 0.048, and 0.023 s, respectively. Also, the average settling times under case 2 are 0.061 s for the SMC method, 0.21 s for the PI, and 0.12 s for the PSO-PI method. This analysis shows that the suggested BES is the faster approach, which enhances the BLDC motor's response.

- ✓ Steady-state error: The simulation results explicitly indicate the remarkable effectiveness of the BES algorithm in removing the steady-state error of the speed. Consequently, the end tracking error remains exceedingly near zero, regardless of the load conditions being at the nominal level or under variations, thus verifying the excellent level of accuracy attained. The overshoot and undershoot in the motor's speed are canceled, and the steady state error in the speed is very low when compared to the other techniques, especially the PI and PSO-PI methods.
- ✓ Robustness: All methods used in the study are assessed with three case studies for checking the robustness of the controller by subjecting it to different situations. These included sudden changes in the load torque, along with variations of the speed reference. The BES-based controller reveals an excellent level of robustness even with the presence of system perturbations.

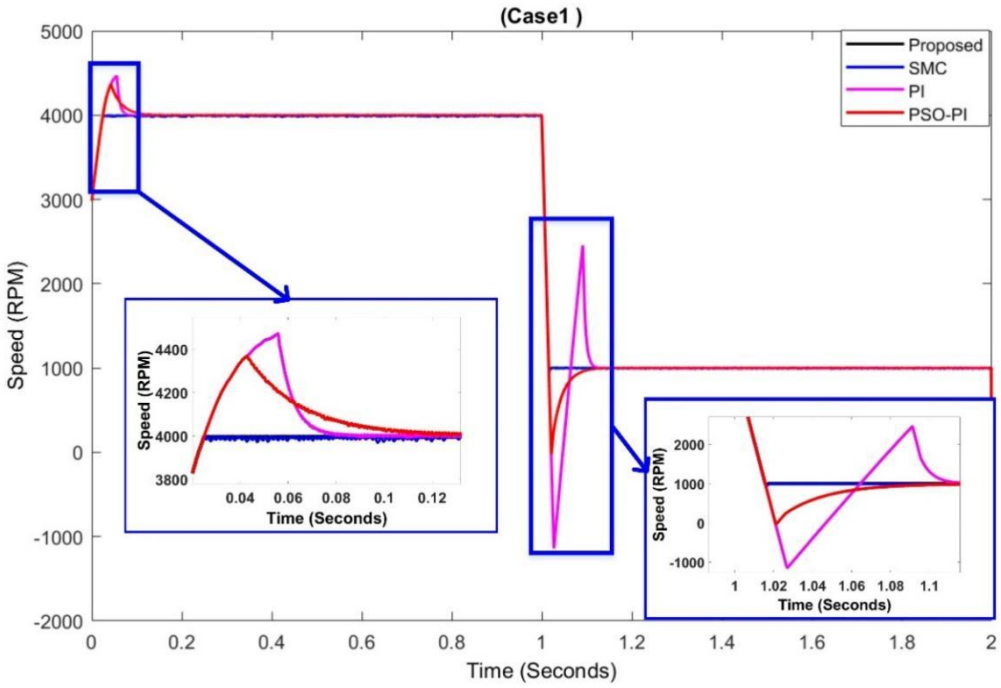

Figure 11. Comparison between the proposed method and existing methods under case study 1.

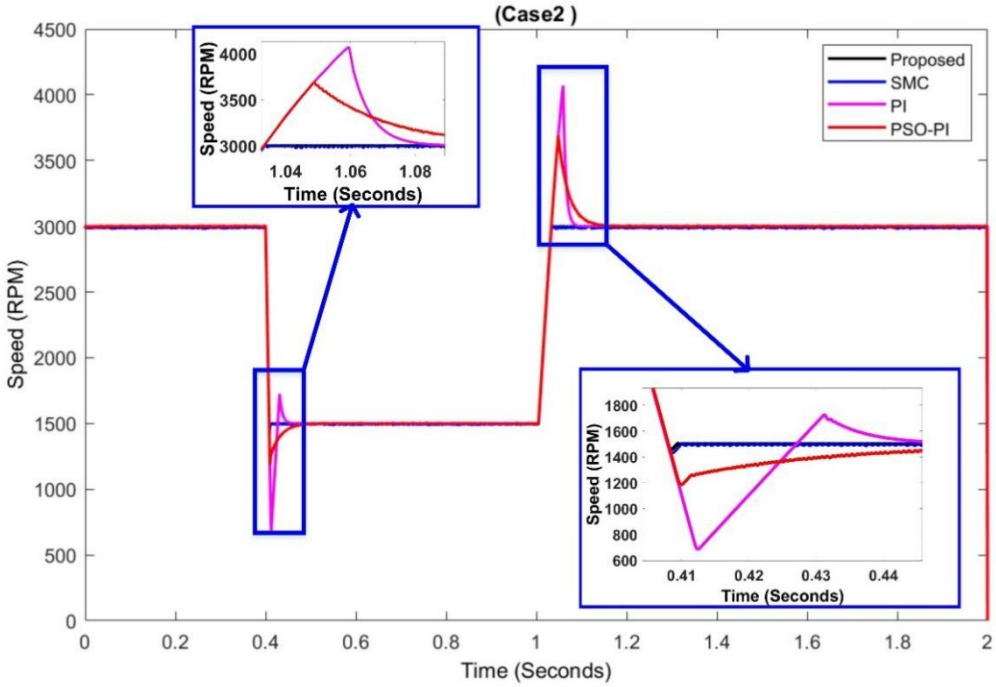

Figure 12. Comparison between the proposed method and existing methods under case study 2.

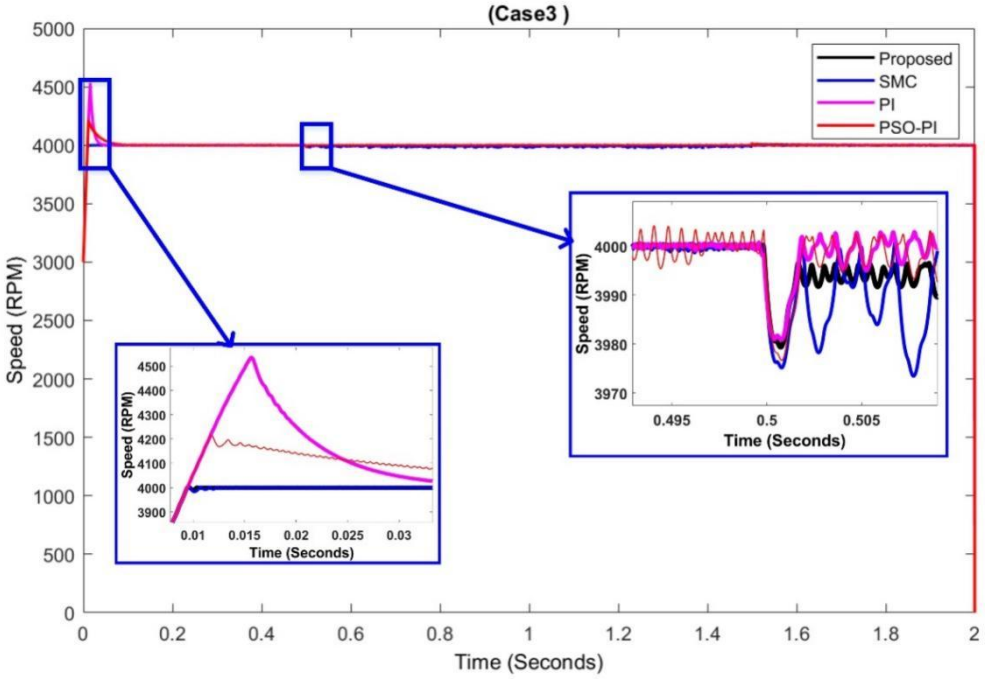

Figure 13. Comparison between the proposed method and existing methods under case study 3.

Table 3. Numerical results and comparisons between the suggested method and existing methods.

Cases	Metric	Proposed	SMC [36]	PI [37]	PSO-PI [38]
Case 1	Rise time (s)	0.01	0.012	0.04	0.02
	Settling time (s)	0.05	0.055	0.2	0.1
	Overshoot (%)	0	0	30	15
	Undershoot (%)	0	0	35	20
	Stability	Highly stable	Stable	Oscillatory	Moderately stable
Case 2	Rise time (s)	0.012	0.016	0.05	0.024
	Settling time (s)	0.06	0.07	0.25	0.16
	Overshoot (%)	0	0	30	18
	Undershoot (%)	0	0	34	24
	Stability	Highly stable	Stable	Oscillatory	Moderately stable
Case 3	Rise time (s)	0.01	0.02	0.056	0.027
	Settling time (s)	0.03	0.06	0.2	0.1
	Overshoot (%)	0	1	25	15
	Undershoot (%)	2	6	5	10
	Stability	Stable	Oscillatory	Oscillatory	Moderately stable

5. Conclusions and future work

In conclusion, this paper presents a new control strategy for controlling the BLDC motor using the bald eagle search (BES) algorithm for optimal tuning of the proportional-integral (PI) controller. The BLDC motor is analyzed mathematically and then implemented using MATLAB/Simulink environment. The hysteresis current control is used, and the BES–PI control is applied as a speed controller. The BES–PI controller, through gain scheduling that performed PI tuning, optimized the dynamics of performance limitation experienced with classical PI control. Simulation results based on three case studies proved that the BES–PI controller outperformed the traditional PI, SMC, and PSO-PI methods in terms of settling time, rise time, and overshoot. Therefore, the proposed method demonstrated a fast rise time of approximately 0.015 s, zero overshoot, and a minimum settling time of 0.03 s, which was measured as the fastest among the tested methods. These findings validate that the proposed method provides a rapid response, precise speed command execution, and effective disturbance rejection. The control performance for transients and steady states is improved significantly with the application of BES in the tuning of PI, which renders BES–PI controllers suitable for real-time, high-precision BLDC motor drives. Future work will provide the hardware implementation of the suggested control method on a physical motor prototype to test and verify its real-time effectiveness and prove the reliability of the control under different load conditions.

Author contributions

Arwa Amer Abdulkareem: Conceptualization, Methodology, Data curation, Formal analysis, Writing – original draft, and Writing – review & editing; Salam J. Yaqoob: Methodology: Data curation, Software, Validation; Ietiqal M. Alwan: Methodology, Resources, and Formal analysis.

Use of Generative-AI tools declaration

The authors declare they have not used Artificial Intelligence (AI) tools in the creation of this article.

Conflict of interest

The authors declare there is no conflict of interest in this paper.

References

1. Neethu U, Jisha VR (2012) Speed control of Brushless DC Motor: A comparative study. In *2012 IEEE international conference on power electronics, drives and energy systems (PEDES)*, 1–5. https://doi.org/10.1109/PEDES.2012.6484349
2. Suganthi P, Nagapavithra S, Umamaheswari S (2017) Modeling and simulation of closed loop speed control for BLDC motor. In *2017 Conference on Emerging Devices and Smart Systems (ICEDSS)*, 229–233. https://doi.org/10.1109/ICEDSS.2017.8073686
3. MadhusudhanaRao G, SankerRam BV, Kumar BS, Kumar KV (2010) Speed control of BLDC motor using DSP. *International Journal of Engineering Science and Technology* 2: 143–147. https://doi.org/10.1109/TSSA56819.2022.10063899
4. Walekar VR, Murkute SV (2018) Speed control of BLDC motor using PI & Fuzzy approach: a comparative study. In *2018 International Conference on Information, Communication, Engineering and Technology (ICICET)*, 1–4. https://doi.org/10.1109/ICICET.2018.8533723
5. Mamadapur A, Mahadev GU (2019) Speed control of BLDC motor using neural network controller and PID controller. In *2019 2nd international conference on power and embedded drive control (ICPEDC)*, 146–151. https://doi.org/10.1109/ICPEDC47771.2019.9036695
6. Wu HC, Wen MY, Wong CC (2016) Speed control of BLDC motors using hall effect sensors based on DSP. In *2016 International Conference on System Science and Engineering (ICSSE)*, 1–4. https://doi.org/10.1109/ICSSE.2016.7551633
7. Alsayid B, Salah WA, Alawneh Y (2019) Modelling of sensored speed control of BLDC motor using MATLAB/SIMULINK. *International Journal of Electrical and Computer Engineering* 9: 3333. https://doi.org/10.11591/ijece.v9i5.pp3333-3343
8. Kristiyono R, Wiyono W (2021) Autotuning fuzzy PID controller for speed control of BLDC motor. *Journal of Robotics and Control (JRC)* 2: 400–407. https://doi.org/10.18196/jrc.25114
9. Kumarasamy V, KarumanchettyThottam Ramasamy V, Chandrasekaran G, Chinnaraj G, Sivalingam P, Kumar NS (2023) A review of integer order PID and fractional order PID controllers using optimization techniques for speed control of brushless DC motor drive. *Int J Syst Assur Eng* 14: 1139–1150. https://doi.org/10.1007/s13198-023-01952-x
10. Megrini M, Gaga A, Mehdaoui Y (2024) Processor in the loop implementation of artificial neural network controller for BLDC motor speed control. *Results in Engineering* 23: 102422. https://doi.org/10.1016/j.rineng.2024.102422
11. Fu J, Gu S, Wu L, Wang N, Lin L, Chen Z (2025) Research on Optimization of Diesel Engine Speed Control Based on UKF-Filtered Data and PSO Fuzzy PID Control. *Processes* 13: 777. https://doi.org/10.3390/pr13030777
12. Maghfiroh H, Ramelan A, Adriyanto F (2022) Fuzzy-PID in BLDC motor speed control using MATLAB/Simulink. *Journal of Robotics and Control (JRC)* 3: 8–13.

https://doi.org/10.18196/jrc.v3i1.10964
13. Dutta P, Nayak SK (2021) Grey wolf optimizer based PID controller for speed control of BLDC motor. *J Electr Eng Technol* 16: 955–961. https://doi.org/10.1007/s42835-021-00660-5
14. Vanchinathan K, Valluvan KR (2018) A metaheuristic optimization approach for tuning of fractional-order PID controller for speed control of sensorless BLDC motor. *J Circuit Syst Comput* 27: 1850123. https://doi.org/10.1142/S0218126618501232
15. Naqvi SSA, Jamil H, Iqbal N, Khan S, Lee DI, Park YC, et al. (2024). Multi-objective optimization of PI controller for BLDC motor speed control and energy saving in Electric Vehicles: A constrained swarm-based approach. *Energy Rep* 12: 402–417. https://doi.org/10.1016/j.egyr.2024.06.019
16. Bazi S, Benzid R, Bazi Y, Rahhal MMA (2021) A fast firefly algorithm for function optimization: application to the control of BLDC motor. *Sensors* 21: 5267. https://doi.org/10.3390/s21165267
17. Vanchinathan K, Valluvan KR, Gnanavel C, Gokul C (2021) Design methodology and experimental verification of intelligent speed controllers for sensorless permanent magnet brushless DC motor: intelligent speed controllers for electric motor. *Int T Electr Energy Syst* 31: e12991. https://doi.org/10.1002/2050-7038.12991
18. Intidam A, El Fadil H, Housny H, El Idrissi Z, Lassioui A, Nady S, et al. (2023) Development and experimental implementation of optimized PI-ANFIS controller for speed control of a brushless DC motor in fuel cell electric vehicles. *Energies* 16: 4395. https://doi.org/10.3390/en16114395
19. Arivalahan R, Venkatesh S, Vinoth T (2022) An effective speed regulation of brushless DC motor using hybrid approach. *Advances in Engineering Software* 174: 103321. https://doi.org/10.1016/j.advengsoft.2022.103321
20. Bogdan V, Adrian M, Leonard L, Alexandra B, Alecsandru S, Ionut N (2021) Design and optimization of a BLDC motor for small power vehicles. In *2021 International Conference on Electromechanical and Energy Systems (SIELMEN)*, 438–443. https://doi.org/10.1109/SIELMEN53755.2021.9600327
21. Shafique F, Fakhar MS, Rasool A, Kashif SAR (2024) Analyzing the performance of metaheuristic algorithms in speed control of brushless DC motor: Implementation and statistical comparison. *Plos one* 19: e0310080. https://doi.org/10.1371/journal.pone.0310080
22. Cui H, Ruan J, Wu C, Zhang K, Li T (2023) Advanced deep deterministic policy gradient based energy management strategy design for dual-motor four-wheel-drive electric vehicle. *Mech Mach Theory* 179: 105119. https://doi.org/10.1016/j.mechmachtheory.2022.105119
23. Jarkas AM, Doss M (2025) Optimized PI controller tuning for improved performance in BLDC motor speed control using heuristic adaptive lyrebird optimization algorithm. *Electrical Engineering*, 1–21. https://doi.org/10.1007/s00202-025-02984-1
24. Çelik E, Karayel M (2024) Effective speed control of brushless DC motor using cascade 1PDf-PI controller tuned by snake optimizer. *Neural Computing and Applications* 36: 7439–7454. https://doi.org/10.1007/s00521-024-09470-y
25. Krishnamoorthy SK, Das N, Gudimetla P, Emami K (2024) Enhanced speed control for BLDC motors using WOA-integrated PID controller optimization. *IEEE Access*. https://doi.org/10.1109/ACCESS.2024.3480349
26. Genc N, Kalimbetova ZS (2024) Cuckoo optimization algorithm based fuzzy logic speed controller for BLDC motor. *Electr Pow Compo Syst* 52: 2065–2077. https://doi.org/10.1080/15325008.2024.2322679
27. Suresh V, Kishore RD, Jahnavi VG, Manjula D, Lokesh M (2025) Interleaved Landsman

Converter with Class Topper Optimized PI Control in Sensorless BLDC Motor Drive for Electric Vehicle. *Проблемы региональной энергетики* 1: 191–203. https://doi.org/10.52254/1857-0070.2025.1-65.14
28. Poudel YK, Bhandari P (2024) Control of the BLDC motor using ant colony optimization algorithm for tuning PID parameters. *Archives of Advanced Engineering Science* 2: 108–113. https://doi.org/10.47852/bonviewAAES32021184
29. Jabari M, Ekinci S, Izci D, Bajaj M, Zaitsev I (2024) Efficient DC motor speed control using a novel multi-stage FOPD-PI controller optimized by the Pelican optimization algorithm. *Scientific Reports* 14: 22442. https://doi.org/10.1038/s41598-024-73409-5
30. Akorede MA, Aborisade DO, Adebayo IG (2025) Speed control enhancement of a brushless direct current motor using transit search optimizer-based proportional integral derivatives controller. *LAUTECH Journal of Engineering and Technology* 19: 221–229. https://doi.org/10.36108/laujet/5202.91.0232
31. Sharma S, Sharma NK, Bajaj M, Kumar V, Jurado F, Kamel S (2022) Optimal BLDC motor control using a WOA-based LQR strategy. In *2022 4th Global Power, Energy and Communication Conference (GPECOM)*, 222–226. https://doi.org/10.1109/GPECOM55404.2022.9815609
32. Thangavelu A, Stephen JE, Samidurai S, Velusamy R, Subramaniyam Sivaraju S, Usha S, et al. (2025) Reduction of Current Harmonics in BLDC Motors Using the Proposed Sigmoid Trapezoidal Current Hysteresis Control. *World Electric Vehicle Journal* 16: 355. https://doi.org/10.1109/GPECOM55404.2022.9815609
33. Usha S, Dubey PM, Ramya R, Suganyadevi MV (2021) Performance enhancement of BLDC motor using PID controller. *International Journal of Power Electronics and Drive Systems* 12: 1335. http://doi.org/10.11591/ijpeds.v12.i3.pp1335-1344
34. El-Shorbagy MA, Bouaouda A, Nabwey HA, Abualigah L, Hashim FA (2024) Bald eagle search algorithm: a comprehensive review with its variants and applications. *Syst Sci Control Eng* 12: 2385310. https://doi.org/10.1080/21642583.2024.2385310
35. Alsattar HA, Zaidan AA, Zaidan BB (2020) Novel meta-heuristic bald eagle search optimisation algorithm. *Artif Intell Rev* 53: 2237–2264. https://doi.org/10.1007/s10462-019-09732-5
36. Hafez AT, Sarhan AA, Givigi S (2019) Brushless DC motor speed control based on advanced sliding mode control (SMC) techniques. In *2019 IEEE International Systems Conference (SysCon)*, 1–6. https://doi.org/10.1109/SYSCON.2019.8836754
37. Mahmud M, Motakabber SMA, Alam AZ, Nordin AN (2020) Adaptive PID controller using for speed control of the BLDC motor. In *2020 IEEE International Conference on Semiconductor Electronics (ICSE)*, 168–171. https://doi.org/10.1109/ICSE49846.2020.9166883
38. Bhandari P, Pancha B, Poudel YK, Lal AK, Chapagain MR, Achary N, et al. (2023) Application of particle swarm optimization (PSO) algorithm for PID parameter tuning in speed control of brushless DC (BLDC) motor. In *Journal of Physics: Conference Series* 2570: 012018. https://doi.org/10.1088/1742-6596/2570/1/012018